

---

# Do Diffusion Models Suffer Error Propagation? Theoretical Analysis and Consistency Regularization

---

Yangming Li, Zhaozhi Qian, Mihaela van der Schaar  
Department of Applied Mathematics and Theoretical Physics  
University of Cambridge  
{y1874, zq224, mv472}@cam.ac.uk

## Abstract

While diffusion models have achieved promising performances in data synthesis, they might suffer *error propagation* because of their *cascade structure*, where the distributional mismatch spreads and magnifies through the chain of denoising modules. However, a strict analysis is expected since many sequential models such as Conditional Random Field (CRF) are free from error propagation. In this paper, we empirically and theoretically verify that diffusion models are indeed affected by error propagation and we then propose a regularization to address this problem. Our theoretical analysis reveals that the question can be reduced to whether every denoising module of the diffusion model is fault-tolerant. We derive insightful transition equations, indicating that the module can't recover from input errors and even propagates additional errors to the next module. Our analysis directly leads to a consistency regularization scheme for diffusion models, which explicitly reduces the distribution gap between forward and backward processes. We further introduce a bootstrapping algorithm to reduce the computation cost of the regularizer. Our experimental results on multiple image datasets show that our regularization effectively handles error propagation and significantly improves the performance of vanilla diffusion models.

## 1 Introduction

As a new generation of generative models, diffusion models [1] outperform classical counterparts like GANs [2] in producing high-quality and diverse data. In spite of their great success, we argue that diffusion models have not reached their full potential due to *error propagation*[3]. The problem stems from the *cascade structure* in a system [3], which involves of a long chain of components connected end-to-end. In this setting, the output error of one component might propagate to the subsequent components such that the error accumulates along the chain. As a result, the last component would generate very inaccurate outputs. For a diffusion model, the modules that sequentially compose its backward process form a cascade structure, and they are not fully precise in denoising. Since the backward process is also very lengthy, the effect of error propagation on diffusion models is potentially significant and worth a careful study.

Does error propagation indeed happen to diffusion models? This question is non-trivial because some sequential models, e.g., Conditional Random Fields (CRFs) [4] and Hidden Markov Models (HMMs) [5], are free from error propagation [6]. One main focus of our work is to empirically and theoretically analyze this question. For the empirical study, we can measure the errors of diffusion models in terms of different denoising iterations (i.e., the quality of latent variables), which are all expected to be zero in an ideal situation.

To theoretically analyze error propagation in diffusion models, we investigate whether every denoising module in the model is *fault-intolerant*, which we find is crucial in determining whether error

propagation occurs. Our analysis produces a set of transition equations that describe the behavior of the test-time input error as it propagates through the denoising module. These equations reveal that the denoising module cannot correct errors from previous modules and instead amplifies and introduces its own prediction error into the input error of the next module. Therefore, we conclude that the fault intolerance of denoising modules leads to error propagation in diffusion models.

To address the issue of error propagation, we propose a general approach based on our theoretical study. Our approach directly reduces the distribution gap between the synthetic and real samples via an additional regularization term during training. This approach enables joint optimization of all denoising modules in the model by exposing them to errors from preceding modules, leading to generated data that is more distributionally consistent with real samples. However, a challenge is that obtaining the precise value of the regularization term is computationally expensive. To overcome this, we propose a bootstrap algorithm inspired by temporal difference (TD) learning [7, 8], which achieves the same goal while maintaining high run-time efficiency. Experimental results on multiple image datasets demonstrate that our approach effectively eliminates error propagation in diffusion models, improving their performance in image generation.

**Contributions.** This paper makes three main contributions. We provide the first solid *empirical evidence* that error propagation affects diffusion models and our findings highlight an avenue for improving diffusion models. Secondly, our *theoretical analysis* establishes that the denoising modules of the model are fault-intolerant, which is the root-cause of the error propagation phenomenon. Finally, to mitigate error propagation, we propose a novel computationally feasible regularization method that directly reduces the distribution gap between synthetic and real samples in the backward process. Experiments on multiple image datasets show that our approach effectively eliminates error propagation in diffusion models and improves their performance in image generation.

## 2 Background: Diffusion Model

In this section, we briefly review the mainstream architecture of diffusion models (i.e., DDPM). A diffusion model consists of two Markov chains of  $T$  steps. One is the forward process (also known as the *diffusion process*), which incrementally adds Gaussian noises into real sample  $\mathbf{x}_0$ , which is a  $K$ -dimensional vector, drawn from the distribution  $q(\mathbf{x}_0)$ . In this process, a sequence of latent variables  $\mathbf{x}_{1:T} = [\mathbf{x}_1, \mathbf{x}_2, \dots, \mathbf{x}_T]$  are generated in order and the last one  $\mathbf{x}_T$  approximately follows a standard Gaussian:

$$q(\mathbf{x}_{1:T} | \mathbf{x}_0) = \prod_{t=1}^T q(\mathbf{x}_t | \mathbf{x}_{t-1}), \quad q(\mathbf{x}_t | \mathbf{x}_{t-1}) = \mathcal{N}(\mathbf{x}_t; \sqrt{1 - \beta_t} \mathbf{x}_{t-1}, \beta_t \mathbf{I}), \quad (1)$$

where  $\mathcal{N}$  denotes a Gaussian distribution and  $\mathbf{I}$  represents an identity matrix.  $\beta_t, 1 \leq t \leq T$ , represents a predefined variance schedule.

The other is the backward process, a reverse version of the forward process (hence it is also called the *reverse process*). Specifically, the process first draws an initial sample  $\mathbf{x}_T$  from standard Gaussian distribution  $p(\mathbf{x}_T) = \mathcal{N}(\mathbf{0}, \mathbf{I})$  and then gradually denoises it into a sequence of latent variables  $\mathbf{x}_{T-1:0} = [\mathbf{x}_{T-1}, \mathbf{x}_{T-2}, \dots, \mathbf{x}_0]$  in reverse order:

$$p_\theta(\mathbf{x}_{T:0}) = p(\mathbf{x}_T) \prod_{t=T}^1 p_\theta(\mathbf{x}_{t-1} | \mathbf{x}_t), \quad p_\theta(\mathbf{x}_{t-1} | \mathbf{x}_t) = \mathcal{N}(\mathbf{x}_{t-1}; \boldsymbol{\mu}_\theta(\mathbf{x}_t, t), \sigma_t \mathbf{I}), \quad (2)$$

where  $p_\theta(\mathbf{x}_{t-1} | \mathbf{x}_t)$  denotes a backward module with parameters  $\theta$  shared across different iterations to fit posterior probability  $q(\mathbf{x}_{t-1} | \mathbf{x}_t)$ , and  $\sigma_t \mathbf{I}$  is a predefined covariance matrix.

The expected negative log-likelihood  $\mathbb{E}[-\log p_\theta(\mathbf{x}_0)]$  is treated as the loss function for optimizing diffusion models. Since the exact log-likelihood is computationally intractable, common practices apply Jensen’s inequality to derive its upper bound:

$$\begin{aligned} \mathbb{E}_{\mathbf{x}_0 \sim q(\mathbf{x}_0)}[-\log p_\theta(\mathbf{x}_0)] &\leq \mathcal{L}^{\text{nl}} = \mathbb{E}_q[D_{\text{KL}}(q(\mathbf{x}_T | \mathbf{x}_0) || p(\mathbf{x}_T))] + \mathbb{E}_q[-\log p_\theta(\mathbf{x}_0 | \mathbf{x}_1)] \\ &\quad + \sum_{1 \leq t < T} \mathbb{E}_q[D_{\text{KL}}(q(\mathbf{x}_{t-1} | \mathbf{x}_t, \mathbf{x}_0) || p_\theta(\mathbf{x}_{t-1} | \mathbf{x}_t))] \end{aligned}, \quad (3)$$

where  $D_{\text{KL}}$  denotes the KL divergence. Every term of this approximate loss has an analytic form making it feasible for computation. [9] further applied reparameterization tricks to the loss  $\mathcal{L}^{\text{nl}}$  to

reduce its estimation variance. For example, the mean  $\boldsymbol{\mu}_\theta$  is formulated by

$$\boldsymbol{\mu}_\theta(\mathbf{x}_t, t) = \frac{1}{\sqrt{\bar{\alpha}_t}} \left( \mathbf{x}_t - \frac{\beta_t}{\sqrt{1 - \bar{\alpha}_t}} \boldsymbol{\epsilon}_\theta(\mathbf{x}_t, t) \right), \quad (4)$$

in which  $\alpha_t = 1 - \beta_t$ ,  $\bar{\alpha}_t = \prod_{t'=1}^t \alpha_{t'}$ , and  $\boldsymbol{\epsilon}_\theta$  is parameterized by a neural network. Under this scheme, the loss  $\mathcal{L}^{\text{nl}}$  can be simplified as

$$\mathcal{L}^{\text{nl}} = \sum_{t=1}^T \underbrace{\mathbb{E}_{\mathbf{x}_0 \sim q(\mathbf{x}_0), \boldsymbol{\epsilon} \sim \mathcal{N}(\mathbf{0}, \mathbf{I})} \left[ \|\boldsymbol{\epsilon} - \boldsymbol{\epsilon}_\theta(\sqrt{\bar{\alpha}_t} \mathbf{x}_0 + \sqrt{1 - \bar{\alpha}_t} \boldsymbol{\epsilon}, t)\|^2 \right]}_{\mathcal{L}_t^{\text{nl}}}, \quad (5)$$

where the neural network  $\boldsymbol{\epsilon}_\theta$  is tasked to fit Gaussian noise  $\boldsymbol{\epsilon}$ .

### 3 Error Propagation

In this section, we give a formal definition of *error propagation*, a preview of its mathematical formulation, and explain why diffusion models are possibly affected by this phenomenon. Error propagation is a classical concept in engineering practices (e.g., computer networks) [3, 10, 11], which impacts some models of a *cascade structure*. Given a model that consists of multiple series-connected components. This problem is triggered by two conditions:

**Inaccurate Modules** Every component is not precise in converting its input into the output. Hence, the inputs to all components, except for the first one, might contain errors.

**Fault Intolerance** Each component of the model is not capable of recovering from such errors. As a result, the errors are spread and magnified along the chain.

The diffusion model obviously has a cascade structure, and its component  $p_\theta(\mathbf{x}_{t-1} | \mathbf{x}_t), t \in [1, T]$  (i.e., denoising module), which is trained from limited data, likely has output errors in practice. Therefore, diffusion models might suffer error propagation based on the first condition. This claim is uncertain because it's unclear whether denoising modules can inherently correct the errors from other components (i.e., fault tolerance).

The mathematical formulation of error propagation highly depends on specific systems and the error definition. For example, the error might be defined at the sample level (e.g., the probability that one chain model to fail in processing a sample) [10], unlike our paper that will define it at the distribution level. Therefore, we first conceptualize the two conditions as above and then formulate them in the next section. A preview is as follows. We will first define the error metric for every denoising module  $p_\theta(\mathbf{x}_{t-1} | \mathbf{x}_t)$  as its distribution gap  $\eta D_{\text{KL}}(p_\theta(\mathbf{x}_{t-1} | \mathbf{x}_t) || q(\mathbf{x}_{t-1} | \mathbf{x}_t))$  to the approximation goal (i.e., inverse forward probability)  $q(\mathbf{x}_{t-1} | \mathbf{x}_t)$ , where  $\eta$  is some scale constant; Then, by defining the input distribution error to the component  $p_\theta(\mathbf{x}_{t-1} | \mathbf{x}_t)$  as  $\mu_t$ , we will infer that it contributes to an error increase as  $\mu_{t-1} - \mu_t$  to the next denoising module  $p_\theta(\mathbf{x}_{t-2} | \mathbf{x}_{t-1})$  because its output is the input to the next component. Therefore, we assert that the module  $q(\mathbf{x}_{t-1} | \mathbf{x}_t)$  is fault-intolerant if  $\mu_{t-1} - \mu_t \geq \eta D_{\text{KL}}(p_\theta(\mathbf{x}_{t-1} | \mathbf{x}_t) || q(\mathbf{x}_{t-1} | \mathbf{x}_t))$ , which means the component makes the propagated error even worse rather than reducing it. In our analysis at the next section, we will see how to define propagation error  $\mu_t$  in Eq. (8) and scale  $\eta$  in Eq. (13).

While the second condition is commonly ignored [12, 13], we argue that it's worth serious verification. In fact, many sequential models are free from error propagation. A typical example is CRF [4], where the prediction errors of its modules don't correlate with their locations in the model. Hence, our work focuses on whether the second condition is met for diffusion models.

### 4 Main Study: Fault Intolerance

In this section, we aim to analyze whether the denoising modules of the diffusion model are *fault-tolerant*. If they do not, based on our pre-analysis in Sec. 3, we can say that error propagation affects the diffusion model by definition.

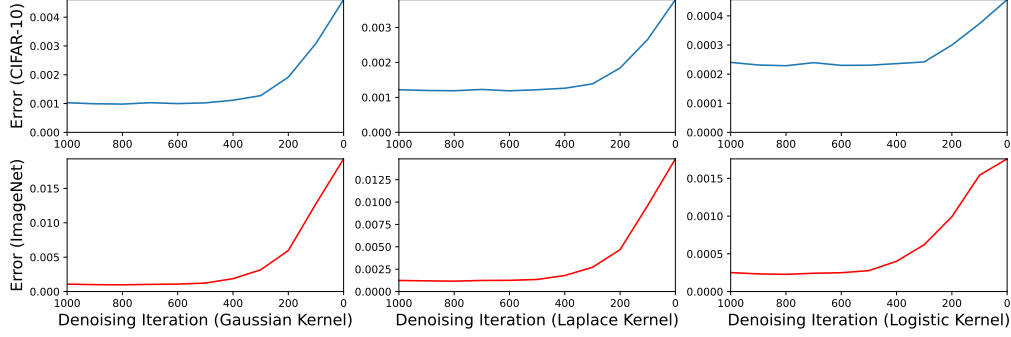


Figure 1: The error (Y-axis) dynamics of diffusion models with respect to denoising iteration  $t$  (X-axis). Every dynamics is estimated in terms of a specific kernel function (e.g., Gaussian) and some dataset (e.g., CIFAR-10). The above results show that *error propagation* happens to the diffusion model and its denoising modules are at least not fully *fault-tolerant*.

#### 4.1 Error Definition

To begin with, we have to formally define “error” for diffusion models, the core concept of error propagation. Note that the loss term  $\mathcal{L}_t^{\text{nil}}$  in Eq. (5) can be reformulated as

$$\mathcal{L}_t^{\text{nil}} = \mathbb{E}_{\mathbf{x}_0 \sim q(\mathbf{x}_0), \mathbf{x}_t \sim q(\mathbf{x}_t | \mathbf{x}_0)} \left[ \left\| \frac{\mathbf{x}_t - \sqrt{\bar{\alpha}_t} \mathbf{x}_0}{\sqrt{1 - \bar{\alpha}_t}} - \epsilon_\theta(\mathbf{x}_t, t) \right\|^2 \right],$$

by denoting the term  $\sqrt{\bar{\alpha}_t} \mathbf{x}_0 + \sqrt{1 - \bar{\alpha}_t} \epsilon$  as  $\mathbf{x}_t$  based on a fact [9]:  $q(\mathbf{x}_t | \mathbf{x}_0) = \mathcal{N}(\mathbf{x}_t; \sqrt{\bar{\alpha}_t} \mathbf{x}_0, (1 - \bar{\alpha}_t) \mathbf{I})$ . From this equality, we can see that, at training time, the input  $\mathbf{x}_t$  to the module  $p_\theta(\mathbf{x}_{t-1} | \mathbf{x}_t)$  follows a fixed distribution that is specified by the forward process  $q$ :

$$\int_{\mathbf{x}_0} q(\mathbf{x}_0) q(\mathbf{x}_t | \mathbf{x}_0) d\mathbf{x}_0 = \int_{\mathbf{x}_0} q(\mathbf{x}_t, \mathbf{x}_0) = q(\mathbf{x}_t), \quad (6)$$

which is inconsistent with the variational distribution that the module  $p_\theta(\mathbf{x}_{t-1} | \mathbf{x}_t)$  receives from its previous denoising iteration  $t + 1$  during evaluation:

$$\int_{\mathbf{x}_{T:t+1}} p(\mathbf{x}_T) \prod_{i=T}^{t+1} p_\theta(\mathbf{x}_{i-1} | \mathbf{x}_i) d\mathbf{x}_{T:t+1} = \int_{\mathbf{x}_{T:t+1}} p_\theta(\mathbf{x}_t, \mathbf{x}_{T:t+1}) d\mathbf{x}_{T:t+1} = p_\theta(\mathbf{x}_t). \quad (7)$$

From these results, we can see that the discrepancy between these two distributions,  $q(\mathbf{x}_t)$  and  $p_\theta(\mathbf{x}_t)$ , causes the denoising module  $p_\theta(\mathbf{x}_{t-1} | \mathbf{x}_t)$  to receive distributionally inconsistent inputs at training and evaluation times. This discrepancy is actually the error contained in the test-time inputs to the module  $p_\theta(\mathbf{x}_{t-1} | \mathbf{x}_t)$ , so we have the following definition.

**Definition 4.1** (General Error Measure). For a standard diffusion model, the input error at test time to its module  $p_\theta(\mathbf{x}_{t-1} | \mathbf{x}_t)$  is measured as the discrepancy between *marginal backward distribution*  $p_\theta(\mathbf{x}_t)$  and *marginal forward distribution*  $q(\mathbf{x}_t)$ . We formulate this measure as

$$\mathcal{D}_f(t) = f(p_\theta(\mathbf{x}_t), q(\mathbf{x}_t)), T \geq t \geq 0, \quad (8)$$

where  $f$  is an appropriate functional that takes two probabilistic distributions as the inputs and measures their symmetric or asymmetric distance.

*Remark 4.1.* The use of functional  $f$  is to estimate the distribution gap: its value becomes larger (or smaller) when the input two distributions get more different (or closer). There are many commonly used candidates. For example, KL divergence and cross entropy [14].

*Remark 4.2.* Measure  $\mathcal{D}_f(t)$  indicates not only the input errors that the module  $p_\theta(\mathbf{x}_{t-1} | \mathbf{x}_t)$  receives from its previous modules but also reflects the quality of the latent variable  $\mathbf{x}_t$  generated by the backward process. For example, when  $t = 0$ , term  $\mathcal{D}_f(0)$  tells whether the generated samples are distributionally consistent with real data.

In the following, we will empirically and theoretically specify the dynamics of error  $\mathcal{D}_f(t)$  over denoising iteration  $t$  with selective functional  $f$ . With the dynamics, we can verify whether and explain why denoising module  $p_\theta(\mathbf{x}_{t-1} | \mathbf{x}_t)$  is fault-intolerant.

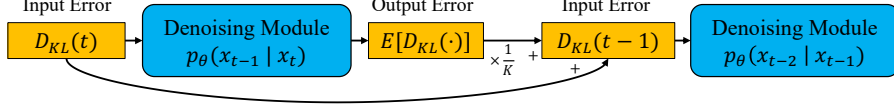


Figure 2: The illustration of our theoretical discovery, i.e., Theorem 4.1: every denoising module  $p_\theta(\mathbf{x}_{t-1} | \mathbf{x}_t)$  of a diffusion model can't reduce the error  $\mathcal{D}_{\text{KL}}(t)$  that it receives from previous modules, and transfers the error together with its own prediction error  $\mathbb{E}[D_{\text{KL}}(p_\theta(\mathbf{x}_{t-1} | \mathbf{x}_t) || q(\mathbf{x}_{t-1} | \mathbf{x}_t))]$  into the input error  $\mathcal{D}_{\text{KL}}(t-1)$  to the next module  $p_\theta(\mathbf{x}_{t-2} | \mathbf{x}_{t-1})$ . Based on our pre-analysis in Sec. 3, we can say module  $p_\theta(\mathbf{x}_{t-1} | \mathbf{x}_t)$  is fault-intolerant, and hence error propagation happens to diffusion models by definition.

## 4.2 Empirical Error Estimation

Prior to theoretical analysis, we directly estimate error  $\mathcal{D}_f(t)$  for all denoising iterations  $[T, T-1, \dots, 1]$  to show its dynamics. Like CRF, if diffusion models are not affected by error propagation, the dynamics of  $\mathcal{D}_f(t)$  should appear as a horizontal line with slight fluctuations.

Since marginal distributions,  $p_\theta(\mathbf{x}_t)$  and  $q(\mathbf{x}_t)$ , have no closed-form solutions, most functionals are not feasible for empirical estimations (i.e., calculations based on samples), including the KL-divergence and cross entropy. An exception is the maximum mean discrepancy (MMD) [15]. With MMD, error  $\mathcal{D}_f(t)$  can be specifically formulated as an expectation:

$$\mathcal{D}_{\text{MMD}}(t) = \|\mathbb{E}_{\mathbf{x}_t \sim p_\theta(\mathbf{x}_t)}[\phi(\mathbf{x}_t)] - \mathbb{E}_{\mathbf{x}_t \sim q(\mathbf{x}_t)}[\phi(\mathbf{x}_t)]\|_{\mathcal{H}}, \quad (9)$$

where  $\mathcal{H}$  denotes a reproducing kernel Hilbert space and  $\phi: \mathbb{R}^K \rightarrow \mathcal{H}$  is a feature map. The square of term  $\mathcal{D}_f(t)$  has an unbiased estimate as

$$\begin{aligned} \mathcal{D}_{\text{MMD}}(t)^2 \approx & \frac{1}{N^2} \sum_{1 \leq i, j \leq N} \mathcal{K}(\mathbf{x}_t^{\text{back}, i}, \mathbf{x}_t^{\text{back}, j}) + \frac{1}{M^2} \sum_{1 \leq i, j \leq M} \mathcal{K}(\mathbf{x}_t^{\text{forw}, i}, \mathbf{x}_t^{\text{forw}, j}) \\ & - \frac{2}{NM} \sum_{1 \leq i \leq N, 1 \leq j \leq M} \mathcal{K}(\mathbf{x}_t^{\text{back}, i}, \mathbf{x}_t^{\text{forw}, j}) \end{aligned}, \quad (10)$$

where the operation  $\mathbf{x}_t^{\text{back}, i} \sim p_\theta(\mathbf{x}_t)$ ,  $1 \leq i \leq N$  is performed in terms of Eq. (2), the operation  $\mathbf{x}_t^{\text{back}, j} \sim q(\mathbf{x}_t)$ ,  $1 \leq j \leq M$  is done by Eq. (1), and the kernel function  $\mathcal{K}(\cdot)$  simplifies the computations of inner products among  $\{\mathbf{x}_t^{\text{back}, 1}, \mathbf{x}_t^{\text{back}, 2}, \dots, \mathbf{x}_t^{\text{back}, N}, \mathbf{x}_t^{\text{forw}, 1}, \mathbf{x}_t^{\text{forw}, 2}, \dots, \mathbf{x}_t^{\text{forw}, M}\}$ .

We train standard diffusion models [9] on two datasets: CIFAR-10 [16] and Imagenet [17], and adopt three different kernel functions (e.g., Laplace kernel) to compute error  $\mathcal{D}_{\text{MMD}}(t)$ . We also set both  $N$  and  $M$  as 1000. The results are illustrated in Fig. 1, showing that error  $\mathcal{D}_{\text{MMD}}(t)$  rapidly grows as the denoising iteration  $t$  starts from  $T$  to 1, which clearly shows that diffusion models exhibit a phenomenon of error propagation.

Our empirical results in Fig. 1 indicate that the denoising module  $p_\theta(\mathbf{x}_{t-1} | \mathbf{x}_t)$  is not robust to errors propagated from its previous modules. Otherwise, the dynamics of error  $\mathcal{D}_{\text{MMD}}(t)$  won't have such a clear uptrend. However, we can't resort to these uptrends to say that module  $p_\theta(\mathbf{x}_{t-1} | \mathbf{x}_t)$  is totally fault-intolerant. It may just be not robust enough. In the upcoming theoretical analysis, we will exactly prove the fault intolerance of module  $p_\theta(\mathbf{x}_{t-1} | \mathbf{x}_t)$ .

## 4.3 Theoretical Error Analysis

In this part, we prove that every module  $p_\theta(\mathbf{x}_{t-1} | \mathbf{x}_t)$ ,  $1 \leq t \leq T$  is fault-intolerant, thus allowing us to assert that diffusion models suffer error propagation by definition.

To derive analytic error measure  $\mathcal{D}_f(t)$ , we respectively choose KL divergence and cross entropy as functional  $f$  because they are analytically convenient and the theorem of diffusion models is mostly based on KL-divergence (e.g., loss derivation). The resulting measures,  $\mathcal{D}_{\text{KL}}(t)$  and  $\mathcal{D}_{\text{CE}}(t)$ , are as

$$\begin{cases} \mathcal{D}_{\text{KL}}(t) = \frac{1}{K} D_{\text{KL}}(p_\theta(\mathbf{x}_t) || q(\mathbf{x}_t)) = \frac{1}{K} \int_{\mathbf{x}_t} p_\theta(\mathbf{x}_t) \ln \frac{p_\theta(\mathbf{x}_t)}{q(\mathbf{x}_t)} d\mathbf{x}_t \\ \mathcal{D}_{\text{CE}}(t) = \frac{1}{K} D_{\text{CE}}(p_\theta(\mathbf{x}_t) || q(\mathbf{x}_t)) = -\frac{1}{K} \int_{\mathbf{x}_t} p_\theta(\mathbf{x}_t) \ln q(\mathbf{x}_t) d\mathbf{x}_t \end{cases}. \quad (11)$$

The two error types are closely related. It's easy to see that equality  $\mathcal{D}_{\text{KL}}(t) = -(1/K)\mathcal{H}(p_\theta(\mathbf{x}_t)) + \mathcal{D}_{\text{CE}}(t)$  holds, where  $\mathcal{H}(\cdot)$  denotes the differential entropy.  $\mathcal{D}_{\text{KL}}(t)$  differs from  $\mathcal{D}_{\text{CE}}(t)$  in that the minimum of  $\mathcal{D}_{\text{KL}}(t)$  is calibrated as 0. In Sec. A of the supplement, we will prove  $\mathcal{D}_{\text{KL}}(t) = 0, \forall t \in [0, T]$  is achievable in an ideal situation: the diffusion model is *perfectly optimized*.

We formulate the analytic dynamics of error measures as the transition equations between  $\mathcal{D}_f(t)$  and  $\mathcal{D}_f(t+1)$ . Actually, we have the following conclusion.

**Theorem 4.1** (Transition Properties). *For a standard diffusion model, suppose the output of its neural network  $\epsilon_\theta(\cdot)$ , as defined in Eq. (4), follows a standard Gaussian regardless of the input distribution. Then, the cross-entropy error  $\mathcal{D}_{\text{CE}}(t), \forall t \in [1, T]$  satisfies*

$$\mathcal{D}_{\text{CE}}(t-1) = \mathcal{D}_{\text{CE}}(t) + \frac{1}{K} \mathbb{E}_{\mathbf{x}_t \sim p_\theta(\mathbf{x}_t)} [D_{\text{KL}}(p_\theta(\mathbf{x}_{t-1} | \mathbf{x}_t) || q(\mathbf{x}_{t-1} | \mathbf{x}_t))] + C_t, \quad (12)$$

where  $C_t$  is a tiny constant and satisfies  $\lim_{t \rightarrow \infty} t|C_t| = 0$ . Hence, another form of this equality is  $\mathcal{D}_{\text{CE}}(t-1) = \mathcal{D}_{\text{CE}}(t) + (\mathbb{E}[\cdot]/K) + o(1/t)$ . Under proper conditions (e.g., the entropy of distribution  $p_\theta(\mathbf{x}_t)$  is non-increasing with decreasing iteration  $t$ ), then we have

$$\mathcal{D}_{\text{KL}}(t-1) \geq \mathcal{D}_{\text{KL}}(t) + \frac{1}{K} \mathbb{E}_{\mathbf{x}_t \sim p_\theta(\mathbf{x}_t)} [D_{\text{KL}}(p_\theta(\mathbf{x}_{t-1} | \mathbf{x}_t) || q(\mathbf{x}_{t-1} | \mathbf{x}_t))]. \quad (13)$$

Based on this inequality, an immediate corollary is that  $\mathcal{D}_{\text{KL}}(t-1) \geq \mathcal{D}_{\text{KL}}(t)$ .

*Proof.* A complete proof is provided in Sec. B of the supplement. □

*Remark 4.3.* The theorem is based on two main intuitive assumptions: 1) From Eq. (5), we can see that neural network  $\epsilon_\theta$  aims to fit Gaussian noise  $\epsilon$ , and is shared by all denoising iterations, which means that it takes the input from various distributions  $[q(\mathbf{x}_T), q(\mathbf{x}_{T-1}), \dots, q(\mathbf{x}_1)]$ . Therefore, it's reasonable to assume that the output of neural network  $\epsilon_\theta$  follows a standard Gaussian distribution, independent of the input distribution; 2) The backward process is designed to incrementally denoise Gaussian noise  $\mathbf{x}_T \sim \mathcal{N}(\mathbf{0}, \mathbf{I})$  into real sample  $\mathbf{x}_0$ . Ideally, the uncertainty (i.e., noise level) of distribution  $p_\theta(\mathbf{x}_t)$  gradually decreases in that denoising process. From this view, it makes sense to assume that differential entropy  $H_{p_\theta}(\mathbf{x}_t)$  reduces with decreasing iteration  $t$ .

*Remark 4.4.* Since denoising module  $p_\theta(\mathbf{x}_{t-1} | \mathbf{x}_t)$  is supposed to approximate inverse forward probability  $q(\mathbf{x}_{t-1} | \mathbf{x}_t)$ , we interpret term  $\mathbb{E}_{\mathbf{x}_t \sim p_\theta(\mathbf{x}_t)}[\cdot]$  in the above equations as its own prediction error, which is different from the input error  $\mathcal{D}_f(t)$  to the module.

**Discussion on the theoretical results.** Based on Eq. (13), our formal analysis of error propagation in diffusion models can be summarized. The inequality reveals that module  $p_\theta(\mathbf{x}_{t-1} | \mathbf{x}_t)$  not only fails to recover from the error  $\mathcal{D}_{\text{KL}}(t)$  but also incorporates its own prediction error  $\mathbb{E}_{\mathbf{x}_t \sim p_\theta(\mathbf{x}_t)}[\cdot]$  into the input error  $\mathcal{D}_{\text{KL}}(t-1)$  for the subsequent module  $p_\theta(\mathbf{x}_{t-2} | \mathbf{x}_{t-1})$ . Consequently, module  $p_\theta(\mathbf{x}_{t-1} | \mathbf{x}_t)$  is fault-intolerant. Otherwise, we would observe  $\mathcal{D}_{\text{KL}}(t-1) < \mathcal{D}_{\text{KL}}(t) + (1/K)\mathbb{E}[\cdot]$ , indicating a certain level of robustness of the module towards its input error  $\mathcal{D}_{\text{KL}}(t)$ . Building upon this discovery and our preliminary analysis in Sec. 3, we can state that error propagation is an inherent characteristic of diffusion models.

**Connections to empirical estimation.** We used MMD error  $\mathcal{D}_{\text{MMD}}(t)$  instead of KL divergence  $\mathcal{D}_{\text{KL}}(t)$  for empirical error estimation since the latter involves density estimation, which is computationally infeasible for discrete-time diffusion models (i.e., DDPM). While MMD and KL divergence are different approaches to measure the distribution gaps, some previous work [18] proved that KL-divergence can be bounded by MMD from the below and above. In other words, they are like the concept of equivalent norm such that we can expect them to exhibit similar dynamics over decreasing denoising iterations (e.g., uptrends) under the effect of error propagation. Therefore, our results in Fig. 1 are also applicable to error measure  $\mathcal{D}_{\text{KL}}(t)$ .

**Other functional candidates for analysis.** Besides KL-divergence, we also examined several other functionals of F-divergence (e.g., Rényi divergence [19]), but found that only with KL-divergence could we derive some interpretable theoretical results to explain error propagation. This finding is in line with existing works - most theorems about diffusion models are constructed by the log function (e.g., log-likelihood) and KL-divergence.

## 5 Method: Efficient Regularization

Based on the above analysis, we first introduce a basic version of our approach to the problem of error propagation, which covers our core idea but is not practical in terms of running time. Then, we extend this approach to practical use through bootstrapping.

### 5.1 Consistency Regularization

A possible way to handle error propagation for diffusion models is to directly minimize the error measure  $\mathcal{D}_f(t)$  defined in Eq. (8), which means to generalize denoising module  $p_\theta(\mathbf{x}_{t-1} | \mathbf{x}_t)$  to marginal backward distribution  $p_\theta(\mathbf{x}_t)$ . As a result, the module will be robust to the test-time errors caused by the inconsistency between  $p_\theta(\mathbf{x}_t)$  and  $q(\mathbf{x}_t)$ .

For computational feasibility, we adopt MMD as functional  $f$ , which leads to another objective function to train diffusion models:

$$\mathcal{L}_t^{\text{reg}} = \mathcal{D}_{\text{MMD}}(t), \quad \mathcal{L}^{\text{reg}} = \sum_{t=0}^{T-1} w_t \mathcal{L}_t^{\text{reg}}, \quad (14)$$

where  $w_t \propto \exp(\rho * (T - t))$ ,  $\rho \in \mathbb{R}^+$  and  $\sum_{t=0}^{T-1} w_t = 1$ . We exponentially schedule weight  $w_t$  because Fig. 1 suggests that error propagation is more severe as  $t$  gets closer to 0. Term  $\mathcal{L}_t^{\text{reg}}$  is estimated by Eq. (10) in practice, with backward variable  $\mathbf{x}_t^{\text{back},i}$  denoised from a Gaussian noise via Eq. (2) and forward variable  $\mathbf{x}_t^{\text{forw},j}$  converted from a real sample with Eq. (1). Notably, some previous work [18] proved that KL-divergence can be bounded by MMD from the below and above. Therefore, minimising MMD error  $\mathcal{D}_{\text{MMD}}(t)$  is equivalent to minimizing the upper bound of KL-divergence error  $\mathcal{D}_{\text{KL}}(t)$ .

The new loss  $\mathcal{L}^{\text{reg}}$  is in addition to the old one  $\mathcal{L}^{\text{nil}}$  previously defined in Eq. (5) for regularizing the optimization of diffusion models. We linearly combine them as  $\mathcal{L} = \lambda^{\text{nil}} \mathcal{L}^{\text{nil}} + \lambda^{\text{reg}} \mathcal{L}^{\text{reg}}$ , where  $\lambda^{\text{nil}}, \lambda^{\text{reg}} \in (0, 1)$  and  $\lambda^{\text{nil}} + \lambda^{\text{reg}} = 1$ , for joint optimization.

### 5.2 Bootstrap Approximation

A great challenge of applying our approach in practice is the inefficient backward process. Specifically, to sample backward variable  $\mathbf{x}_t^{\text{back},i}$  for estimating loss  $\mathcal{L}_t^{\text{reg}}$ , we have to iteratively apply a sequence of denoising modules  $[p_\theta(\mathbf{x}_{T-1} | \mathbf{x}_T), p_\theta(\mathbf{x}_{T-2} | \mathbf{x}_{T-1}), \dots, p_\theta(\mathbf{x}_t | \mathbf{x}_{t+1})]$  to cast a Gaussian noise into that variable. In the worst case, the neural network  $\epsilon_\theta$  shared by all denoising modules will be called  $T$  times, which is extremely time-consuming.

Inspired by temporal difference (TD) learning [7], we bootstrap the computation of variable  $\mathbf{x}_t^{\text{back},i}$  for efficiency. Normally, this variable is gradually denoised from a Gaussian noise  $\mathbf{x}_T^{\text{back},i} \sim \mathcal{N}(\mathbf{0}, \mathbf{I})$ . For our approach, we first select one variable  $\mathbf{x}_s^{\text{back},i}$ ,  $s > t$  from that denoising process, and apply marginal forward distribution  $q(\mathbf{x}_t)$  to estimate it in a possibly biased manner:

$$\tilde{\mathbf{x}}_s^{\text{back},i} = \sqrt{\bar{\alpha}_s} \mathbf{x}_0 + \sqrt{1 - \bar{\alpha}_s} \boldsymbol{\epsilon}, \quad \mathbf{x}_0 \sim q(\mathbf{x}_0), \quad \boldsymbol{\epsilon} \sim \mathcal{N}(\mathbf{0}, \mathbf{I}), \quad (15)$$

based on a nice property [9] of the forward process:  $q(\mathbf{x}_t | \mathbf{x}_0) = \mathcal{N}(\mathbf{x}_t; \sqrt{\bar{\alpha}_t} \mathbf{x}_0, (1 - \bar{\alpha}_t) \mathbf{I})$ . Here operation  $\sim q(\mathbf{x}_0)$  means to sample from training data, and  $s \sim \mathcal{U}\{\min(t + L, T), t + 1\}$ , where  $L \ll T$  is a predefined sampling length. Then, we apply a list of denoising modules  $[p_\theta(\mathbf{x}_{s-1} | \mathbf{x}_s), p_\theta(\mathbf{x}_{s-2} | \mathbf{x}_{s-1}), \dots, p_\theta(\mathbf{x}_t | \mathbf{x}_{t+1})]$  to iteratively update  $\tilde{\mathbf{x}}_s^{\text{back},i}$  into an alternative  $\tilde{\mathbf{x}}_t^{\text{back},i}$  to variable  $\mathbf{x}_t^{\text{back},i}$ . Each update can be formulated as

$$\tilde{\mathbf{x}}_{k-1}^{\text{back},i} = \frac{1}{\sqrt{\alpha_k}} \left( \tilde{\mathbf{x}}_k^{\text{back},i} - \frac{\beta_k}{\sqrt{1 - \bar{\alpha}_k}} \boldsymbol{\epsilon}_\theta(\tilde{\mathbf{x}}_k^{\text{back},i}, k) \right) + \sigma_k \boldsymbol{\epsilon}, \quad \boldsymbol{\epsilon} \sim \mathcal{N}(\mathbf{0}, \mathbf{I}), \quad (16)$$

where  $t + 1 \leq k \leq s$ . Finally, we apply the alternative  $\tilde{\mathbf{x}}_t^{\text{back},i}$  for computing loss  $\mathcal{L}_t^{\text{reg}}$  in terms of Eq. (10), with at most  $L \ll T$  runs of neural network  $\epsilon_\theta$ .

There is in fact a trade-off between approximation accuracy and time efficiency for specifying sampling length  $L$ . For example, large  $L$  reduces the negative impact from biased initialization  $\tilde{\mathbf{x}}_s^{\text{back},i}$  but incurs a high time cost. We will study this problem in the experiment and also put the details of our training procedure in Sec. D of the supplement.

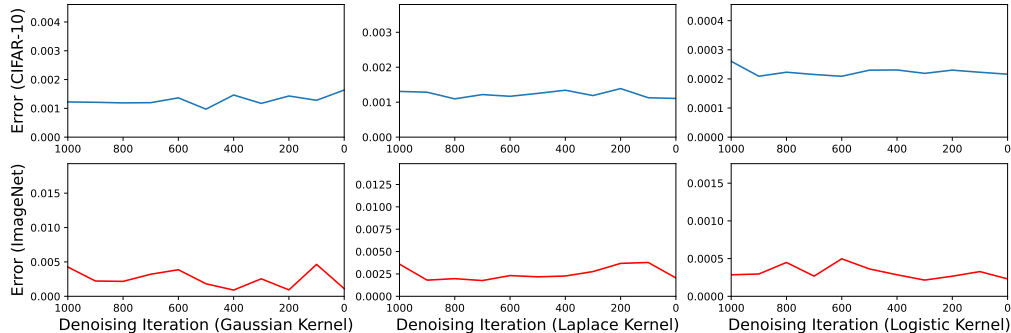


Figure 3: Re-estimated dynamics of the input error  $\mathcal{D}_{\text{MMD}}(t)$  to denoising module  $p_{\theta}(\mathbf{x}_{t-1} | \mathbf{x}_t)$  after applying our regularization  $\mathcal{L}_t^{\text{reg}}$  to its optimization. These dynamics should be compared with those in Fig. 1, showing that we have well handled error propagation.

## 6 Related Work

Diffusion models, due to their superior performances in image synthesis, have received wide attention from the research community of generative models. Despite their great success, diffusion models suffer some problems (e.g., inference efficiency) inherent in their design. Some works tried to address these problems. For instance, [20] facilitated conditional image generation for the diffusion model without resorting to an additional image classifier. This paper is a special study on the structural risk of diffusion models, which receives less attention from recent works.

The topic of this work is also closely related to a problem called exposure bias that occurs to some sequence models [12, 21], which means that a model only exposed to ground truth inputs might not be robust to errors during evaluation. [13] studied this problem for diffusion models due to their sequential structure. However, they lack a solid explanation of why the models are not robust to exposure bias, which is very important because many sequence models (e.g., CRF) is free from this problem. Our analysis in Sec. 4 actually answers that question with empirical evidence and theoretical analysis. More importantly, we argue that their approach, which adds an extra Gaussian noise into the model input, is not an ideal solution, since this simple perturbation certainly can't simulate the complex errors at test time. We have also treated their approach as a baseline and shown that our regularization significantly outperforms it in experiments (Section 7).

There are also some seemingly related papers (e.g., consistency models [22]), which in fact belong to very different research topics (e.g., theoretical convergence [23]) from our paper. We make detailed comparisons between them and our work in Sec. C of the appendix.

## 7 Experiments

We have performed extensive experiments to verify the effectiveness of the proposed approach. Besides special studies (e.g., effect of some hyper-parameter), our main experiments include: 1) By comparing with Fig. 1, we show that the phenomenon of error propagation disappears after applying our regularization to diffusion models; 2) On three image datasets (CIFAR-10, CelebA, and ImageNet), our approach notably improves the performances of diffusion models.

### 7.1 Settings

We evaluate the effectiveness of our approach on three image datasets: CIFAR-10 [16], ImageNet [17], and CelebA [24], with image shapes respectively as  $32 \times 32$ ,  $32 \times 32$ , and  $64 \times 64$ . Following previous works [9, 25], we adopt Frechet Inception Distance (FID) [26] as the evaluation metric. The configuration of our model follows common practices, we adopt U-Net [27] as the backbone and respectively set hyper-parameters  $T, \sigma_t, L, \lambda^{\text{reg}}, \lambda^{\text{nl}}, \rho$  as 1000,  $\beta_t, 5, 0.2, 0.8, 0.003$ . All our model run on 2 ~ 4 Tesla V100 GPUs and are trained within two weeks.



Approach	CIFAR-10 (32 × 32)	ImageNet (32 × 32)	CelebA (64 × 64)
ADM-IP [13]	3.25	2.72	1.31
DDPM [9]	3.61	3.62	1.73
DDPM w/ Consistency Reg.	<b>2.93</b>	<b>2.55</b>	<b>1.22</b>

Table 1: FID scores of our model and baselines on different image datasets. The improvements of our approach over baselines are statistically significant with  $p < 0.01$  under t-test.

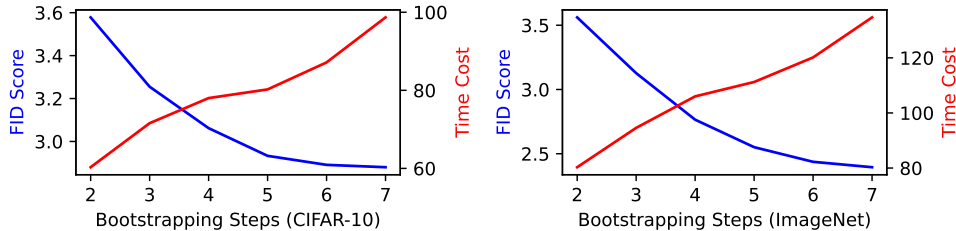


Figure 4: A trade-off study of hyper-parameter  $L$  (i.e., the number of bootstrapping steps) on two datasets. The results show that, as  $L$  gets larger, the model performance limitedly increases while the time cost (measured in seconds) boundlessly grows.

## 7.2 Consistency Regularization Reduces Error Propagation

To show the effect of our regularization  $\mathcal{L}^{\text{reg}}$  to diffusion models, we re-estimate the dynamics of MMD error  $\mathcal{D}_{\text{MMD}}(t)$ , with the same experiment setup of datasets and kernel functions as our empirical study in Sec. 4.2. The only difference is that the input distribution to module  $p_{\theta}(\mathbf{x}_{t-1} | \mathbf{x}_t)$  at training time is no longer  $q(\mathbf{x}_t)$ , but we can still correctly estimate error  $\mathcal{D}_{\text{MMD}}(t)$  with Eq. (10) by re-defining  $\mathbf{x}_t^{\text{forw},j}$  as the training-time inputs the module.

Fig. 3 shows the results. Compared with the uptrend dynamics of vanilla diffusion models in Fig. 1, we can see that the new ones are more like a slightly fluctuating horizontal line, indicating that: 1) every denoising module  $p_{\theta}(\mathbf{x}_{t-1} | \mathbf{x}_t)$  has become robust to inaccurate inputs since error measure  $\mathcal{D}_{\text{MMD}}(t)$  is not correlated with its location  $t$  in the diffusion model; 2) By applying our regularization  $\mathcal{L}^{\text{reg}}$ , the diffusion model is not affected by error propagation anymore.

## 7.3 Performances of Image Generation

The FID scores of our model and baselines on 3 datasets are demonstrated in Table 1. The results of last two rows are obtained by our experiments and those of the first row are copied from [13]. We draw two conclusions from the table: 1) Our regularization notably improves the performances of DDPM, a mainstream architecture of diffusion models, with reductions of FID scores as 18.83% on CIFAR-10, 29.55% on ImageNet, and 29.47% on CelebA. Therefore, handling error propagation benefits in improving the generation quality of diffusion models; 2) Our model significantly outperforms ADM-IP, the baseline that reduces the exposure bias by input perturbation, on all datasets. For example, our FID score on CIFAR-10 are lower than its score by 9.84%. An important factor contributing to our much better performances is that, unlike the baseline, our approach doesn't impose any assumption on the distribution form of propagating errors.

Approach	CIFAR-10 (32 × 32)	CelebA (64 × 64)
DDPM w/ Consistency Reg.	<b>2.93</b>	<b>1.22</b>
Our Model w/o Exponential Schedule $w_t$	3.12	1.35
Our Model w/o Warm-start $\tilde{\mathbf{x}}_s^{\text{back},i}$ ( $L = 5$ )	3.38	1.45
Our Model w/o Warm-start $\tilde{\mathbf{x}}_s^{\text{back},i}$ ( $L = 7$ )	3.15	1.27

Table 2: Ablation studies of two techniques, the schedule of loss weight  $w_t$  and the warm-start initialization of alternative representation  $\tilde{\mathbf{x}}_s^{\text{back},i}$ , used in our approach.

## 7.4 Trade-off Study

The number of bootstrapping steps  $L$  is a key hyper-parameter in our proposed regularization. Its value determination involves a trade-off between effectiveness (i.e., the quality of alternative backward variable  $\tilde{\mathbf{x}}_t^{\text{back},i}$ ) and run-time efficiency.

Fig. 4 shows how FID scores (i.e., model performances) and the averaged time costs of one training step change with respect to different bootstrapping steps  $L$ . For both CIFAR-10 and ImageNet, we can see that, as the number of steps  $L$  increases, FID scores decrease and tend to converge while time costs boundlessly grow. In practice, we set  $L$  as 5 for our model since this configuration leads to good enough performances and incur relatively low time costs.

## 7.5 Ablation Experiments

To make our regularization  $\mathcal{L}^{\text{reg}}$  work in practice, we exponentially schedule weight  $w_t, 0 \leq t < T$  and specially initialize alternative backward variable  $\tilde{\mathbf{x}}_s^{\text{back},i}$  via Eq. (15). Table 2 demonstrates the ablation studies of these two techniques. For the weighted schedule, we can see from the second row that model performances are notably degraded by replacing it with equal weight  $w_t = 1/T$ . Firstly, by adopting random initialization instead of Eq. (15), the model performances drastically decrease, implying that it's necessary to have a warm start; Secondly, the impact of initialization can be reduced by using a larger number of bootstrapping steps  $L$ .

## 8 Conclusion

*Error propagation* is a well-known phenomenon in engineering practices, which happens to many sequence models. Since diffusion models are of a *cascade structure*, a natural question is whether diffusion models are affected by this phenomenon. In the context that some sequence models (e.g., CRF) are free from error propagation, this work provides a solid analysis to answer this question with empirical and theoretical results. Based on our analysis, we propose a consistency regularization to better optimize diffusion models, and improve its efficiency through bootstrapping. We have also conducted extensive experiments to verify the effectiveness of our approach.

Besides popular DDPM and natural images, a lot of variants of diffusion models have emerged and they are applied to different data modalities. Variants include DDIM [28], Latent Diffusion [29], Diffusion Normalizing Flow [30], Variational Diffusion Models [31], etc. and explored data types involve natural language [32], audio [33], time series [34], tabular data [35], etc. Since these variants are still of a cascade structure, future works can apply our analysis to get similar theoretical results and adopt our regularization for performance improvements.

## References

- [1] Jascha Sohl-Dickstein, Eric Weiss, Niru Maheswaranathan, and Surya Ganguli. Deep unsupervised learning using nonequilibrium thermodynamics. In *International Conference on Machine Learning*, pages 2256–2265. PMLR, 2015.
- [2] Ian Goodfellow, Jean Pouget-Abadie, Mehdi Mirza, Bing Xu, David Warde-Farley, Sherjil Ozair, Aaron Courville, and Yoshua Bengio. Generative adversarial nets. In Z. Ghahramani, M. Welling, C. Cortes, N. Lawrence, and K.Q. Weinberger, editors, *Advances in Neural Information Processing Systems*, volume 27. Curran Associates, Inc., 2014.
- [3] Adilson E Motter and Ying-Cheng Lai. Cascade-based attacks on complex networks. *Physical Review E*, 66(6):065102, 2002.
- [4] John Lafferty, Andrew McCallum, and Fernando CN Pereira. Conditional random fields: Probabilistic models for segmenting and labeling sequence data. 2001.
- [5] Lawrence Rabiner and Biinghwang Juang. An introduction to hidden markov models. *iee assp magazine*, 3(1):4–16, 1986.

- [6] Daniel Andor, Chris Alberti, David Weiss, Aliaksei Severyn, Alessandro Presta, Kuzman Ganchev, Slav Petrov, and Michael Collins. Globally normalized transition-based neural networks. In *Proceedings of the 54th Annual Meeting of the Association for Computational Linguistics (Volume 1: Long Papers)*, pages 2442–2452, Berlin, Germany, August 2016. Association for Computational Linguistics.
- [7] Gerald Tesauro et al. Temporal difference learning and td-gammon. *Communications of the ACM*, 38(3):58–68, 1995.
- [8] Ian Osband, Charles Blundell, Alexander Pritzel, and Benjamin Van Roy. Deep exploration via bootstrapped dqn. *Advances in neural information processing systems*, 29, 2016.
- [9] Jonathan Ho, Ajay Jain, and Pieter Abbeel. Denoising diffusion probabilistic models. *Advances in Neural Information Processing Systems*, 33:6840–6851, 2020.
- [10] Xiuwen Fu, Pasquale Pace, Gianluca Aloï, Lin Yang, and Giancarlo Fortino. Topology optimization against cascading failures on wireless sensor networks using a memetic algorithm. *Computer Networks*, 177:107327, 2020.
- [11] Paolo Crucitti, Vito Latora, and Massimo Marchiori. Model for cascading failures in complex networks. *Physical Review E*, 69(4):045104, 2004.
- [12] Wen Zhang, Yang Feng, Fandong Meng, Di You, and Qun Liu. Bridging the gap between training and inference for neural machine translation. In *Proceedings of the 57th Annual Meeting of the Association for Computational Linguistics*, pages 4334–4343, Florence, Italy, July 2019. Association for Computational Linguistics.
- [13] Mang Ning, Enver Sangineto, Angelo Porrello, Simone Calderara, and Rita Cucchiara. Input perturbation reduces exposure bias in diffusion models. *arXiv preprint arXiv:2301.11706*, 2023.
- [14] Solomon Kullback and Richard A Leibler. On information and sufficiency. *The annals of mathematical statistics*, 22(1):79–86, 1951.
- [15] Arthur Gretton, Karsten M Borgwardt, Malte J Rasch, Bernhard Schölkopf, and Alexander Smola. A kernel two-sample test. *The Journal of Machine Learning Research*, 13(1):723–773, 2012.
- [16] Alex Krizhevsky, Geoffrey Hinton, et al. Learning multiple layers of features from tiny images. 2009.
- [17] Jia Deng, Wei Dong, Richard Socher, Li-Jia Li, Kai Li, and Li Fei-Fei. Imagenet: A large-scale hierarchical image database. In *2009 IEEE conference on computer vision and pattern recognition*, pages 248–255. Ieee, 2009.
- [18] Chong Xiao Wang and Wee Peng Tay. Practical bounds of kullback-leibler divergence using maximum mean discrepancy. *arXiv preprint arXiv:2204.02031*, 2022.
- [19] Tim Van Erven and Peter Harremos. Rényi divergence and kullback-leibler divergence. *IEEE Transactions on Information Theory*, 60(7):3797–3820, 2014.
- [20] Jonathan Ho and Tim Salimans. Classifier-free diffusion guidance. In *NeurIPS 2021 Workshop on Deep Generative Models and Downstream Applications*, 2021.
- [21] Marc’ Aurelio Ranzato, Sumit Chopra, Michael Auli, and Wojciech Zaremba. Sequence level training with recurrent neural networks. *ICLR*, 2016.
- [22] Yang Song, Prafulla Dhariwal, Mark Chen, and Ilya Sutskever. Consistency models. 2023.
- [23] Sitan Chen, Sinho Chewi, Jerry Li, Yuanzhi Li, Adil Salim, and Anru Zhang. Sampling is as easy as learning the score: theory for diffusion models with minimal data assumptions. In *The Eleventh International Conference on Learning Representations*, 2023.
- [24] Ziwei Liu, Ping Luo, Xiaogang Wang, and Xiaoou Tang. Deep learning face attributes in the wild. In *Proceedings of the IEEE international conference on computer vision*, pages 3730–3738, 2015.

- [25] Prafulla Dhariwal and Alexander Nichol. Diffusion models beat gans on image synthesis. In M. Ranzato, A. Beygelzimer, Y. Dauphin, P.S. Liang, and J. Wortman Vaughan, editors, *Advances in Neural Information Processing Systems*, volume 34, pages 8780–8794. Curran Associates, Inc., 2021.
- [26] Martin Heusel, Hubert Ramsauer, Thomas Unterthiner, Bernhard Nessler, and Sepp Hochreiter. Gans trained by a two time-scale update rule converge to a local nash equilibrium. *Advances in neural information processing systems*, 30, 2017.
- [27] Olaf Ronneberger, Philipp Fischer, and Thomas Brox. U-net: Convolutional networks for biomedical image segmentation. In *Medical Image Computing and Computer-Assisted Intervention–MICCAI 2015: 18th International Conference, Munich, Germany, October 5-9, 2015, Proceedings, Part III 18*, pages 234–241. Springer, 2015.
- [28] Jiaming Song, Chenlin Meng, and Stefano Ermon. Denoising diffusion implicit models. In *International Conference on Learning Representations*, 2021.
- [29] Robin Rombach, Andreas Blattmann, Dominik Lorenz, Patrick Esser, and Björn Ommer. High-resolution image synthesis with latent diffusion models. In *Proceedings of the IEEE/CVF Conference on Computer Vision and Pattern Recognition*, pages 10684–10695, 2022.
- [30] Qinsheng Zhang and Yongxin Chen. Diffusion normalizing flow. In A. Beygelzimer, Y. Dauphin, P. Liang, and J. Wortman Vaughan, editors, *Advances in Neural Information Processing Systems*, 2021.
- [31] Diederik P Kingma, Tim Salimans, Ben Poole, and Jonathan Ho. On density estimation with diffusion models. In A. Beygelzimer, Y. Dauphin, P. Liang, and J. Wortman Vaughan, editors, *Advances in Neural Information Processing Systems*, 2021.
- [32] Xiang Lisa Li, John Thickstun, Ishaan Gulrajani, Percy Liang, and Tatsunori Hashimoto. Diffusion-LM improves controllable text generation. In Alice H. Oh, Alekh Agarwal, Danielle Belgrave, and Kyunghyun Cho, editors, *Advances in Neural Information Processing Systems*, 2022.
- [33] Zhifeng Kong, Wei Ping, Jiayi Huang, Kexin Zhao, and Bryan Catanzaro. Diffwave: A versatile diffusion model for audio synthesis. In *International Conference on Learning Representations*, 2021.
- [34] Yusuke Tashiro, Jiaming Song, Yang Song, and Stefano Ermon. Csd: Conditional score-based diffusion models for probabilistic time series imputation. *Advances in Neural Information Processing Systems*, 34:24804–24816, 2021.
- [35] Shuhan Zheng and Nontawat Charoenphakdee. Diffusion models for missing value imputation in tabular data. In *NeurIPS 2022 First Table Representation Workshop*, 2022.
- [36] Yufeng Zhang, Wanwei Liu, Zhenbang Chen, Kenli Li, and Ji Wang. On the properties of kullback-leibler divergence between gaussians. *arXiv preprint arXiv:2102.05485*, 2021.
- [37] Chieh-Hsin Lai, Yuhta Takida, Naoki Murata, Toshimitsu Uesaka, Yuki Mitsufuji, and Stefano Ermon. Regularizing score-based models with score fokker-planck equations. In *NeurIPS 2022 Workshop on Score-Based Methods*, 2022.
- [38] Giannis Daras, Yuval Dagan, Alexandros G Dimakis, and Constantinos Daskalakis. Consistent diffusion models: Mitigating sampling drift by learning to be consistent. *arXiv preprint arXiv:2302.09057*, 2023.
- [39] Chieh-Hsin Lai, Yuhta Takida, Toshimitsu Uesaka, Naoki Murata, Yuki Mitsufuji, and Stefano Ermon. On the equivalence of consistency-type models: Consistency models, consistent diffusion models, and fokker-planck regularization. In *ICML 2023 Workshop on Structured Probabilistic Inference & Generative Modeling*, 2023.
- [40] Holden Lee, Jianfeng Lu, and Yixin Tan. Convergence of score-based generative modeling for general data distributions. In *NeurIPS 2022 Workshop on Score-Based Methods*, 2022.
- [41] Sitan Chen, Sinho Chewi, Holden Lee, Yuanzhi Li, Jianfeng Lu, and Adil Salim. The probability flow ode is provably fast. *arXiv preprint arXiv:2305.11798*, 2023.

## A Ideal Scenario: Zero Error Measure

The error measure based on KL divergence is defined as

$$\mathcal{D}_{\text{KL}}(t) = \frac{1}{K} D_{\text{KL}}(p_\theta(\mathbf{x}_t) \parallel q(\mathbf{x}_t)) = \frac{1}{K} \int_{\mathbf{x}_t} p_\theta(\mathbf{x}_t) \ln \frac{p_\theta(\mathbf{x}_t)}{q(\mathbf{x}_t)} d\mathbf{x}_t, \quad (17)$$

which achieves its minimum 0 exclusively at  $p_\theta(\mathbf{x}_t) = q(\mathbf{x}_t)$ . We show that  $\mathcal{D}_{\text{KL}}(t) = 0, \forall t \in [0, T]$  holds in an ideal situation (i.e., diffusion models are *perfectly optimized*).

**Proposition A.1** (Zero Error Measure). *We say a diffusion model is perfectly optimized if every backward probability  $p_\theta(\mathbf{x}_{t-1} \mid \mathbf{x}_t), 1 \leq t \leq T$  equals its reference  $q(\mathbf{x}_{t-1} \mid \mathbf{x}_t), 1 \leq t \leq T$ . For such a model with  $T \rightarrow \infty$ , we have  $\mathcal{D}_{\text{KL}}(t) = 0, \forall t \in [0, T]$ .*

*Proof.* It suffices to show that  $p_\theta(x_t) = q(x_t), \forall t \in [0, T]$  for perfectly optimized diffusion models. We apply mathematical induction to prove this assertion. Initially, let's check whether this is true at  $t = T$ . Based on a nice property of the forward process [9]:

$$q(\mathbf{x}_t \mid \mathbf{x}_0) = \mathcal{N}(\mathbf{x}_t; \sqrt{\bar{\alpha}_t} \mathbf{x}_0, (1 - \bar{\alpha}_t) \mathbf{I}),$$

we can see that term  $q(\mathbf{x}_T \mid \mathbf{x}_0)$  converges to a normal Gaussian  $\mathcal{N}(\mathbf{0}, \mathbf{I})$  as  $T \rightarrow \infty$  because  $\lim_{T \rightarrow \infty} \sqrt{\bar{\alpha}_T} = 0$ . Also note that  $p_\theta(\mathbf{x}_T) = p(\mathbf{x}_T) = \mathcal{N}(\mathbf{x}_T; \mathbf{0}, \mathbf{I})$ , we have

$$\mathbf{q}(\mathbf{x}_T) = \int_{\mathbf{x}_0} \mathbf{q}(\mathbf{x}_T \mid \mathbf{x}_0) \mathbf{q}(\mathbf{x}_0) d\mathbf{x}_0 = \mathcal{N}(\mathbf{x}_T; \mathbf{0}, \mathbf{I}) \int_{\mathbf{x}_0} \mathbf{q}(\mathbf{x}_0) d\mathbf{x}_0 = p_\theta(\mathbf{x}_T) * 1. \quad (18)$$

Therefore, the initial case is proved. Now, we assume the conclusion holds for  $t$ . Considering the precondition  $p_\theta(\mathbf{x}_{t-1} \mid \mathbf{x}_t) = q(\mathbf{x}_{t-1} \mid \mathbf{x}_t)$ , we have

$$\begin{aligned} p_\theta(\mathbf{x}_{t-1}) &= \int_{\mathbf{x}_t} p_\theta(\mathbf{x}_{t-1}, \mathbf{x}_t) d\mathbf{x}_t = \int_{\mathbf{x}_t} p_\theta(\mathbf{x}_{t-1} \mid \mathbf{x}_t) p_\theta(\mathbf{x}_t) d\mathbf{x}_t \\ &= \int_{\mathbf{x}_t} q(\mathbf{x}_{t-1} \mid \mathbf{x}_t) q(\mathbf{x}_t) d\mathbf{x}_t = \int_{\mathbf{x}_t} q(\mathbf{x}_{t-1}, \mathbf{x}_t) d\mathbf{x}_t = q(\mathbf{x}_{t-1}) \end{aligned}, \quad (19)$$

which proves the case for  $t - 1$ . Overall, assertion  $p_\theta(\mathbf{x}_t) = q(\mathbf{x}_t)$  is true for  $t \in [0, T]$ , and therefore the whole conclusion is proved.  $\square$

## B Proof of Transition Properties

According to the law of total expectation, we have

$$\mathcal{D}_{\text{CE}}(t-1) = \frac{1}{K} \mathbb{E}_{\mathbf{x}_{t-1}} [-\ln q(\mathbf{x}_{t-1})] = \frac{1}{K} \mathbb{E}_{\mathbf{x}_t \sim p_\theta(\mathbf{x}_t)} [\mathbb{E}_{\mathbf{x}_{t-1} \sim p_\theta(\mathbf{x}_{t-1} \mid \mathbf{x}_t)} [-\ln q(\mathbf{x}_{t-1})]]. \quad (20)$$

Note that  $q(\mathbf{x}_{t-1})q(\mathbf{x}_t \mid \mathbf{x}_{t-1}) = q(\mathbf{x}_{t-1}, \mathbf{x}_t) = q(\mathbf{x}_t)q(\mathbf{x}_{t-1} \mid \mathbf{x}_t)$ , we have

$$\begin{aligned} \mathcal{D}_{\text{CE}}(t-1) &= \frac{1}{K} \mathbb{E}_{\mathbf{x}_t \sim p_\theta(\mathbf{x}_t)} \left[ \mathbb{E}_{\mathbf{x}_{t-1} \sim p_\theta(\mathbf{x}_{t-1} \mid \mathbf{x}_t)} \left[ -\ln q(\mathbf{x}_t) - \ln \frac{q(\mathbf{x}_{t-1} \mid \mathbf{x}_t)}{q(\mathbf{x}_t \mid \mathbf{x}_{t-1})} \right] \right] \\ &= \frac{1}{K} \mathbb{E}_{\mathbf{x}_t \sim p_\theta(\mathbf{x}_t)} \left[ -\ln q(\mathbf{x}_t) + \mathbb{E}_{\mathbf{x}_{t-1} \sim p_\theta(\mathbf{x}_{t-1} \mid \mathbf{x}_t)} \left[ -\ln \frac{q(\mathbf{x}_{t-1} \mid \mathbf{x}_t)}{q(\mathbf{x}_t \mid \mathbf{x}_{t-1})} \right] \right]. \quad (21) \\ &= \mathcal{D}_{\text{CE}}(t) + \frac{1}{K} \mathbb{E}_{\mathbf{x}_t \sim p_\theta(\mathbf{x}_t)} \left[ \mathbb{E}_{\mathbf{x}_{t-1} \sim p_\theta(\mathbf{x}_{t-1} \mid \mathbf{x}_t)} \left[ \ln \frac{q(\mathbf{x}_t \mid \mathbf{x}_{t-1})}{q(\mathbf{x}_{t-1} \mid \mathbf{x}_t)} \right] \right] \end{aligned}$$

Now, we focus on the iterated expectations  $\mathbb{E}_{\mathbf{x}_{t+1}}[\mathbb{E}_{\mathbf{x}_t}[\cdot]]$  of the above equality. Based on the definition of KL divergence, it's obvious that

$$\begin{aligned} &\mathbb{E}_{\mathbf{x}_t \sim p_\theta(\mathbf{x}_t)} \left[ \mathbb{E}_{\mathbf{x}_{t-1} \sim p_\theta(\mathbf{x}_{t-1} \mid \mathbf{x}_t)} \left[ \ln \left( \frac{p_\theta(\mathbf{x}_t \mid \mathbf{x}_{t-1})}{q(\mathbf{x}_{t-1} \mid \mathbf{x}_t)} \frac{q(\mathbf{x}_t \mid \mathbf{x}_{t-1})}{p_\theta(\mathbf{x}_{t-1} \mid \mathbf{x}_t)} \right) \right] \right] \\ &= \mathbb{E}_{\mathbf{x}_t \sim p_\theta(\mathbf{x}_t)} \left[ \mathbb{E}_{\mathbf{x}_{t-1} \sim p_\theta(\mathbf{x}_{t-1} \mid \mathbf{x}_t)} \left[ \frac{p_\theta(\mathbf{x}_t \mid \mathbf{x}_{t-1})}{q(\mathbf{x}_{t-1} \mid \mathbf{x}_t)} \right] + \mathbb{E}_{\mathbf{x}_{t-1} \sim p_\theta(\mathbf{x}_{t-1} \mid \mathbf{x}_t)} \left[ \ln \frac{q(\mathbf{x}_t \mid \mathbf{x}_{t-1})}{p_\theta(\mathbf{x}_{t-1} \mid \mathbf{x}_t)} \right] \right]. \quad (22) \\ &= \mathbb{E}_{\mathbf{x}_t \sim p_\theta(\mathbf{x}_t)} [D_{\text{KL}}(\cdot)] + \mathbb{E}_{\mathbf{x}_t \sim p_\theta(\mathbf{x}_t)} \left[ \mathbb{E}_{\mathbf{x}_{t-1} \sim p_\theta(\mathbf{x}_{t-1} \mid \mathbf{x}_t)} \left[ \ln \frac{q(\mathbf{x}_t \mid \mathbf{x}_{t-1})}{p_\theta(\mathbf{x}_{t-1} \mid \mathbf{x}_t)} \right] \right] \end{aligned}$$

We denote term  $\mathbb{E}_{\mathbf{x}_t}[\mathbb{E}_{\mathbf{x}_{t-1} \sim p_\theta(\mathbf{x}_{t-1}|\mathbf{x}_t)}[\cdot]]$  here as  $C_t$  and prove it's a constant. Since distribution  $q(\mathbf{x}_t | \mathbf{x}_{t-1})$  is a predefined multivariate Gaussian, we have

$$\begin{aligned} q(\mathbf{x}_t | \mathbf{x}_{t-1}) &= (2\pi\beta_t)^{-\frac{K}{2}} \exp\left(-\frac{\|\mathbf{x}_t - \sqrt{1-\beta_t}\mathbf{x}_{t-1}\|^2}{2\beta_t}\right) \\ &= (1-\beta_t)^{-\frac{K}{2}} (2\pi\beta_t/(1-\beta_t))^{-\frac{K}{2}} \exp\left(-\frac{\|\mathbf{x}_{t-1} - (\mathbf{x}_t/\sqrt{1-\beta_t})\|^2}{2\beta_t/(1-\beta_t)}\right). \quad (23) \\ &= (1-\beta_t)^{-\frac{K}{2}} \mathcal{N}(\mathbf{x}_{t-1}; \mathbf{x}_t/\sqrt{1-\beta_t}, \beta_t/(1-\beta_t)\mathbf{I}) \end{aligned}$$

With this result and the definition of backward probability  $p_\theta(\mathbf{x}_{t-1} | \mathbf{x}_t)$ , we can convert the constant  $C_t$  into the following form:

$$C_t = \frac{1}{K} \mathbb{E}_{\mathbf{x}_t} \left[ -\mathbb{E}_{\mathbf{x}_{t-1}} \left[ \ln \frac{\mathcal{N}(\mathbf{x}_{t-1}; \boldsymbol{\mu}_\theta(\mathbf{x}_t, t), \sigma_t \mathbf{I})}{\mathcal{N}(\mathbf{x}_{t-1}; \mathbf{x}_t/\sqrt{1-\beta_t}, \beta_t/(1-\beta_t)\mathbf{I})} \right] \right] - \frac{\ln(1-\beta_t)}{2}. \quad (24)$$

Note that term  $\mathbb{E}_{\mathbf{x}_{t-1}}[\cdot]$  essentially represents the KL divergence between two Gaussian distributions, which is said to have a closed-form solution [36]:

$$\begin{aligned} D_{\text{KL}}\left(\mathcal{N}\left(\mathbf{x}_{t-1}; \boldsymbol{\mu}_\theta(\mathbf{x}_t, t), \sigma_t \mathbf{I}\right) \parallel \mathcal{N}\left(\mathbf{x}_{t-1}; \frac{\mathbf{x}_t}{\sqrt{1-\beta_t}}, \frac{\beta_t}{1-\beta_t} \mathbf{I}\right)\right) \\ = \frac{1}{2} \left( K \ln \frac{\beta_t}{(1-\beta_t)\sigma_t} - K + \frac{(1-\beta_t)\sigma_t}{\beta_t} K + \frac{1-\beta_t}{\beta_t} \left\| \frac{\mathbf{x}_t}{\sqrt{1-\beta_t}} - \boldsymbol{\mu}_\theta(\cdot) \right\|^2 \right). \end{aligned}$$

Considering this result, the fact that variance  $\sigma_t$  is primarily set as  $\beta_t$  in DDPM [9], and the definition of mean  $\boldsymbol{\mu}_\theta$ , we can simplify term  $C_t$  as

$$\begin{aligned} C_t &= -\frac{1-\beta_t}{2\beta_t} \mathbb{E}_{\mathbf{x}_t \sim p_\theta(\mathbf{x}_t)} \left[ \left\| \frac{\mathbf{x}_t}{\sqrt{1-\beta_t}} - \boldsymbol{\mu}_\theta(\mathbf{x}_t, t) \right\|^2 \right] + \frac{\beta_t}{2} \\ &= -\frac{\beta_t}{2K(1-\bar{\alpha}_t)} \mathbb{E}_{\mathbf{x}_t \sim p_\theta(\mathbf{x}_t)} [\|\boldsymbol{\epsilon}_\theta(\mathbf{x}_t, t)\|^2] + \frac{\beta_t}{2}. \quad (25) \end{aligned}$$

Considering our assumption that neural network  $\boldsymbol{\epsilon}_\theta$  behaves as a standard Gaussian irrespective of the input distribution, we can interpret term  $\mathbb{E}_{\mathbf{x}_t \sim p_\theta(\mathbf{x}_t)}[\cdot]$  as the total variance of all dimensions of a multivariate normal distribution. Therefore, its value is  $K \times 1$ , the sum of  $K$  unit variances. An additional fact is that the current practice [9] sets variance  $\beta_t$ ,  $1 \leq t \leq T$  as to linearly increase from  $\beta_1 = 10^{-4}$  to  $\beta_T = 0.02$ , so term  $|C_t|$  can be reduced as

$$|C_t| = \frac{\beta_t}{2} \left| 1 - \frac{1}{1-\bar{\alpha}_t} \right| < \left( \frac{1}{t} \right)^{1.01}. \quad (26)$$

Combining this inequality with Eq. (21) and Eq. (22), our first equality in the theorem:

$$\mathcal{D}_{\text{CE}}(t-1) = \mathcal{D}_{\text{CE}}(t) + \frac{1}{K} \mathbb{E}_{\mathbf{x}_t \sim p_\theta(\mathbf{x}_t)} [D_{\text{KL}}(p_\theta(\mathbf{x}_{t-1} | \mathbf{x}_t) \parallel q(\mathbf{x}_{t-1} | \mathbf{x}_t))] + C_t, \quad (27)$$

and its derivation  $\mathcal{D}_{\text{CE}}(t-1) = \mathcal{D}_{\text{CE}}(t) + (\mathbb{E}[\cdot]/K) + o(1/t)$  are both true.

With the above equality, considering  $\mathcal{D}_{\text{KL}}(t) = -(1/K)\mathcal{H}(p_\theta(\mathbf{x}_t)) + \mathcal{D}_{\text{CE}}(t)$  and assuming that the entropy of distribution  $p_\theta(\mathbf{x}_t)$  decreases during the backward process (i.e.,  $H_{p_\theta}(\mathbf{x}_{t-1}) < H_{p_\theta}(\mathbf{x}_t)$ ,  $0 \leq t < T$ ) and the tiny constant  $C_t$  is negligible for such a decrease, we have

$$\begin{aligned} \mathcal{D}_{\text{KL}}(t-1) &\geq -\frac{H_{p_\theta}(\mathbf{x}_t)}{K} + \mathcal{D}_{\text{CE}}(t) + \frac{1}{K} \mathbb{E}_{\mathbf{x}_t} [D_{\text{KL}}(p_\theta(\mathbf{x}_{t-1} | \mathbf{x}_t) \parallel q(\mathbf{x}_{t-1} | \mathbf{x}_t))] \\ &= \mathcal{D}_{\text{KL}}(t) + \frac{1}{K} \mathbb{E}_{\mathbf{x}_t \sim p_\theta(\mathbf{x}_t)} [D_{\text{KL}}(p_\theta(\mathbf{x}_{t-1} | \mathbf{x}_t) \parallel q(\mathbf{x}_{t-1} | \mathbf{x}_t))] \quad (28) \end{aligned}$$

This derivation shows our third assertion in the theorem is true. Another corollary from this inequality is that  $\mathcal{D}_{\text{KL}}(t-1) \geq \mathcal{D}_{\text{KL}}(t)$  since KL divergence is inherently non-negative.

## C Additional References

Some papers [22, 37–39], which aim to improve the estimation of score functions, might seem to be related to us because they are titled with consistency training or regularization. One big difference

between these papers and our work is that they assert without proof that diffusion models are affected by error propagation, while we have empirically and theoretically verified whether this phenomenon happens. Notably, this assertion is not trivial because many sequential models (e.g., CRF and HMM) are free from error propagation. Besides, these papers proposed regularisation methods in light of some expected consistencies. While these methods are similar to our regularisation in name, they were actually to improve the score estimation at every time step (i.e., the prediction accuracy of every component in a sequential model), which differs much from our approach that aims to improve the robustness of score functions to input errors. The key to solving error propagation is to make score functions fault-tolerant (rather than pursuing higher accuracy) [3, 11], because it's very hard to have perfect score functions with limited training data. Therefore, these methods are orthogonal to us in reducing the effect of error propagation and do not constitute ideal solutions to the problem.

Another group of seemingly related papers [23, 40, 41] aim to derive convergence guarantees based on the assumption of bounded score estimation errors. Specifically speaking, these papers analysed how generated samples converge (in distribution) to real data with respect to increasing discretization levels. However, studies [3, 11] on error propagation generally focus on analysing the error dynamics of a chain model over time (i.e., how input errors to the score functions of decreasing time steps evolve). Therefore, these papers are of a very different research theme from our paper. More notably, these papers either assumed bounded score estimation errors or just ignored them, which are actually not appropriate to analyse error propagation for diffusion models. There are two reasons. Firstly, the error dynamics shown in our paper (Fig. 1) have exponentially-like increasing trends, implying that the score functions close to time step 0 are of very poor estimation. Secondly, if all components of a chain model are very accurate (i.e., bounded estimation errors), then the effect of error propagation will be insignificant regardless of whether the components are fault-intolerant. Therefore, it's better to set the estimation errors as uncertain variables for studying error propagation.

## D Training Algorithm

Compared with common practices [9, 28], we additionally regularize diffusion models with MMD error measure  $\mathcal{L}^{\text{reg}}$  for optimization. The details are in Algorithm 1.

---

### Algorithm 1: Optimization with Consistency Regularization

---

**Input:** Batch size  $B$ , number of backward iterations  $T$ , sample range  $L \ll T$ .

**while** *the model is not converged* **do**

Sample a batch of samples from the training set  $\mathcal{S}_0 = \{\mathbf{x}_0^i \mid \mathbf{x}_0^i \sim q(\mathbf{x}_0^i), 1 \leq i \leq T\}$ .

Sample a time point for vanilla training  $t \in \mathcal{U}\{1, T\}$ .

Estimate training loss  $\mathcal{L}_t^{\text{nl}}$  for every real sample  $\mathbf{x}_0^i \in \mathcal{S}_0$ .

Sample a time point for regularization  $s \in \mathcal{U}\{\min(t + L, T), t + 1\}$ .

Sample a new batch of samples from the training set  $\mathcal{S}'_0 = \{\mathbf{x}_0^j \mid \mathbf{x}_0^j \sim q(\mathbf{x}_0^j), 1 \leq j \leq T\}$ .

Sample forward variables  $\mathcal{S}_s^{\text{forw}} = \{\mathbf{x}_s^{\text{forw},j} \mid \mathbf{x}_s^{\text{forw},j} \sim q(\mathbf{x}_s^{\text{forw},j} \mid \mathbf{x}_0^j), \mathbf{x}_0^j \in \mathcal{S}'_0\}$  at step  $s$ .

Sample forward variables  $\mathcal{S}_t^{\text{forw}} = \{\mathbf{x}_t^{\text{forw},i} \mid \mathbf{x}_t^{\text{forw},i} \sim q(\mathbf{x}_t^{\text{forw},i} \mid \mathbf{x}_0^i), \mathbf{x}_0^i \in \mathcal{S}_0\}$  at step  $t$ .

Sample alternative backward variables at time step  $s$  as

$\mathcal{S}_s^{\text{back}} = \{\tilde{\mathbf{x}}_s^{\text{back},i} \mid \tilde{\mathbf{x}}_s^{\text{back},i} \sim p_\theta(\tilde{\mathbf{x}}_s^{\text{back},i} \mid \mathbf{x}_t^{\text{forw},i}), \mathbf{x}_0^i \in \mathcal{S}_t^{\text{forw}}\}$ .

Estimate MMD error measure  $\mathcal{L}_s^{\text{reg}}$  based on  $\mathcal{S}_s^{\text{forw}}$  and  $\mathcal{S}_s^{\text{back}}$ .

Update the model parameter  $\theta$  with gradient  $\nabla_\theta(\lambda^{\text{nl}} \mathcal{L}_t^{\text{nl}} + \lambda^{\text{reg}} w_s \mathcal{L}_s^{\text{reg}})$ .

---